

María J. Uriz · Xavier Turon · Mikel A. Becerro

Silica deposition in Demosponges: spiculogenesis in *Crambe crambe*

Received: 31 March 2000 / Accepted: 19 April 2000 / Published online: 17 June 2000
© Springer-Verlag 2000

Abstract Transmission electron-microscopy images coupled with dispersive X-ray analysis of the species *Crambe crambe* have provided information on the process of silica deposition in Demosponges. Sclerocytes (megasclerocytes) lie close to spicules or surround them at different stages of growth by means of long thin enveloping pseudopodia. Axial filaments occur free in the mesohyl, in close contact with sclerocytes, and are triangular in cross section, with an internal silicified core. The unit-type membrane surrounding the growing spicule coalesces with the plasmalemma. The axial filament of a growing spicule and that of a mature spicule contain 50%–70% Si and 30%–40% Si relative to that contained in the spicule wall, respectively. The extracellular space between the sclerocyte and the growing spicule contains 50%–65%. Mitochondria, vesicles and dense inclusions of sclerocytes exhibit less than 10%. The cytoplasm close to the growing spicule and that far from the growing spicule contain up to 50% and less than 10%, respectively. No Si has been detected in other parts of the sponge. The megascleres are formed extracellularly. Once the axial filament is extruded to the mesohyl, silicification is accomplished in an extracellular space formed by the enveloping pseudopodia of the sclerocyte. Si deposition starts at regularly distributed sites along the axial filament; this may be related to the highly hydroxylated zones of the silicatein- α protein. Si is concentrated in the cytoplasm of the sclerocyte close to the plasmalemma that surrounds the growing spicules. Orthosilicic acid seems to be pumped, both from the meso-

hyl to the sclerocyte and from the sclerocyte to the extracellular pocket containing the growing spicule, via the plasmalemma.

Key words Silica deposition · Spiculogenesis · Microanalysis · Ultrastructure · Sclerocytes · Megascleres · *Crambe crambe* (Demospongiae)

Introduction

The intra- versus extracellular secretion of spicules in Demosponges has been extensively discussed over the last century and is still a matter of speculation (Simpson 1984). Microscleres could be secreted both intra- and extracellularly (Simpson 1968) and most recent studies seem to support the intracellular secretion of megascleres (Garrone 1969; Simpson and Vaccaro 1974; Garrone et al. 1981; Hartman 1981; Bei et al. 1998). However, our current knowledge of spiculogenesis of siliceous sponges is mostly based upon the secretion of microscleres and small megascleres in a few species. It seems physically impossible for a single sponge cell, 20 μm in diameter, to include a large megasclere such as those of Astrophorid, Spirophorid, Hadromerid or some Axinellid sponges. At least in these extreme cases, the involvement of several sclerocytes in secreting a single spicule seems to be necessary and, thus, extracellular secretion cannot be ruled out. As Simpson (1984) has pointed out, an intracellular origin had also been proposed for calcareous sponge spicules (Bogner et al. 1998) before their extracellular origin was fully demonstrated (Ledger 1975; Ledger and Jones 1991; Andral et al. 1998; Angelidis and Aloupi 1998). More research on spicule secretion of taxonomically distant siliceous sponge species is still needed to establish an intra- or extracellular origin of siliceous megascleres or whether both processes occur in different types of spicules.

Controversy also exists as to the form of the axial filament of megascleres in cross section and its implications for spicule symmetry and shape. Light-microscopic

This work was partially sponsored by projects MAS3-PL961088 from the EU, CICYT-MAR98–1004-C02, Generalitat 1999SGR00184, and a Postdoctoral contract to M.B.

M.J. Uriz (✉) · Mikel A. Becerro
Center for Advanced Studies (CSIC),
Camí de Sta. Bàrbara s/n, 17300 Blanes (Girona), Spain
e-mail: Iosune@ceab.csic.es

X. Turon
Department of Animal Biology (Invertebrates),
Faculty of Biology, University of Barcelona,
645 Diagonal Avenue, 08028 Barcelona, Spain

images from a large number of species seem to indicate that most Demosponges have an axial filament with a triangular cross section (Reiswig 1971). Subsequent ultrastructural studies have indicated a hexagonal shape for cross sections of axial filaments in various species of the order Haplosclerida (Garrone 1969; Simpson and Vaccaro 1974; Wilkinson and Garrone 1980; Weissenfels and Langenbruch 1985) and in the Poecilosclerid *Neofibularia irata* (Wilkinson and Garrone 1980). As some of those hexagonal shapes had been viewed as triangular by light microscopy (Reiswig 1971), Garrone et al. (1981) and Simpson (1984) have concluded that all the axial filaments of Demosponge spicules, microscleres included, must be hexagonal in cross section. Although Simpson et al. (1985) have described triangular filaments in desilicified triaenes and oxeas of *Stelletta grubii*, a general hexagonal shape is still assumed by some recent authors (Rützler and Smith 1993).

The mechanism by which silica is concentrated and deposited around the axial filament to form spicules is still poorly known. It has not been shown whether silica is transferred from the water to the inside of the unit-type membrane that wraps the growing spicule by means of vacuoles or directly through the cytoplasm of the sclerocyte. Orthosilicic acid, before it polymerises to SiO₂, may be transferred from the surrounding water to the epithelial cells (pinacocytes or choanocytes), from these cells to the mesohyl and then to the sclerocytes. However, as no silicic acid has been found in pinacocytes or choanocytes (Simpson 1984), it may enter the sponge mesohyl directly through transient spaces between the epithelial cells.

In this study, we have examined spiculogenesis in the Demosponge *Crambe crambe* (Schmidt), a widespread Mediterranean littoral sponge (Uriz et al. 1992), the skeleton of which varies with the geographical locality (Maldonado and Uriz 1996). This species was first described as having styles to subtylostyles as megascleres and asteroid desmas and unguiferous tree-teeth isochelae as microscleres (Thiele 1899). However, desmas and isochelae are rare in most specimens and are lacking in the populations of the Iberian littoral and nearby regions (Bibiloni 1990). Although *Crambe* megascleres are monaxonid-like, they appear to have phylogenetic affinities with polyaxonid sponges (Uriz and Maldonado 1995), which adds interest to the study of their formation.

Materials and methods

Animals

Adult specimens and larvae of *Crambe crambe* were collected at a depth of 4–8 m in the Blanes littoral (NE of the Iberian Peninsula, western Mediterranean) in the summer of 1993.

Transmission electron microscopy

Transmission electron-microscopic (TEM) observations were performed with a Hitachi H600 microscope (Scientific and Technical Services, University of Barcelona). Small samples, 3 mm in diameter, were fixed for 5 h in 2.5% glutaraldehyde in 0.1 M sodium ca-

codylate buffer (osmolarity adjusted to 980 mOsm with saccharose) at 4°C, washed three times in the buffer solution, postfixed for 90 min in 2% osmium tetroxide (OsO₄) in the same buffer, dehydrated in an acetone series and embedded in ERL 4206 (Spurr 1969). Ultrathin sections were contrasted with uranyl acetate and lead citrate (Reynolds 1963). A set of samples was treated with hydrofluoric acid (5%, 2 h) after fixation and prior to embedding to remove the silica. Some samples were specifically stained by the thiocarbohydrazide/silver proteinate reaction (Thiéry technique) to reveal glycogen reserves (Boury-Esnault and Doumenc 1979).

X-ray microanalysis

Microanalysis was performed with a Hitachi H800 MT microscope (Scientific and Technical Services, University of Barcelona). Semi-thin sections (0.5 µm thick) of fixed (glutaraldehyde) and post-fixed (OsO₄) material, not contrasted with uranyl acetate and lead citrate, were mounted on a titanium grid and examined by TEM-coupled energy dispersive X-ray microanalysis for the presence of Si. An acceleration of 100 kV was used in scanning transmission-electron microscopy mode. Electron beam excitation was detected in a thin-window (10 µm²) Kevex detector connected to a Kevex 8000 analytical system with Quantex 6.13 software. We used the Si K_α peak at 1.75 keV as a qualitative indicator of the presence of Si, since it does not overlap with other peaks. The gain rate was adjusted to 1000–2000 count s⁻¹ and the acquisition time was 300 s. The Cl signal from the embedding resin used by some authors (Thompson et al. 1983) as an internal standard was not clear in some of the spectra obtained. Thus, the Ti signal coming from the grid was used as a standard to render comparable the spectra from different cells and compartments and at different magnifications. The presence of the signals corresponding to Si was examined in the spectra obtained. We used the ratio of the Si K_α peak at 1.75 keV to the Ti K_α peak at 4.5 keV as a semi-quantitative measure for comparison of the compartments studied. Values of the Si peak that did not exceed the background level by twice the standard deviation of the background intensity were not considered indicative of the presence of Si (Chapple et al. 1997).

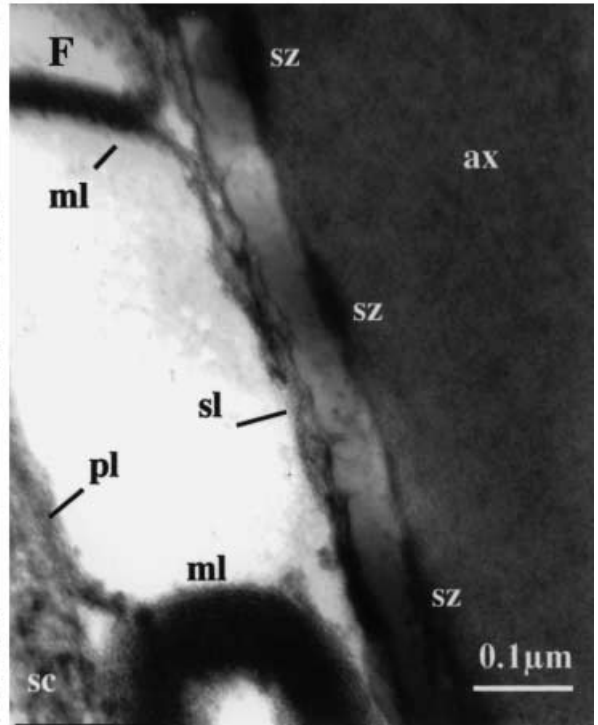
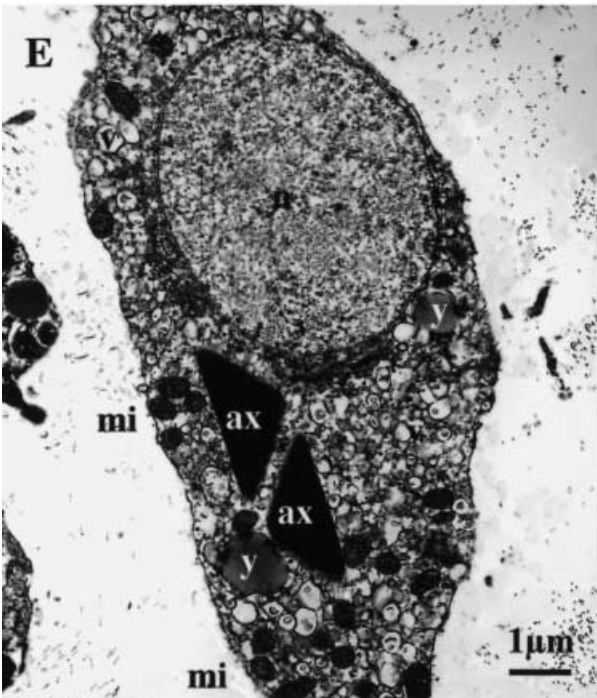
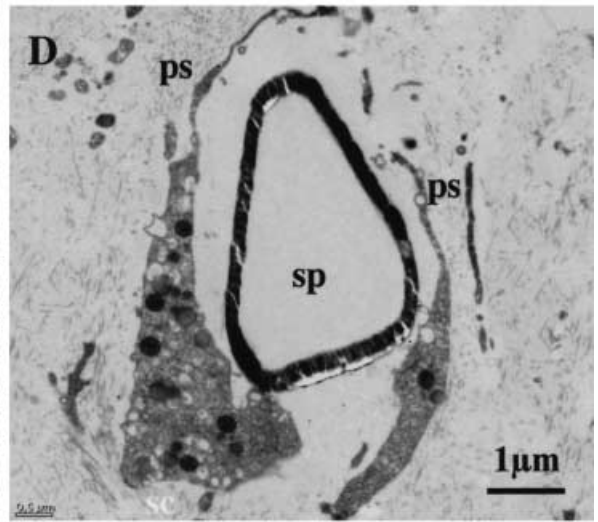
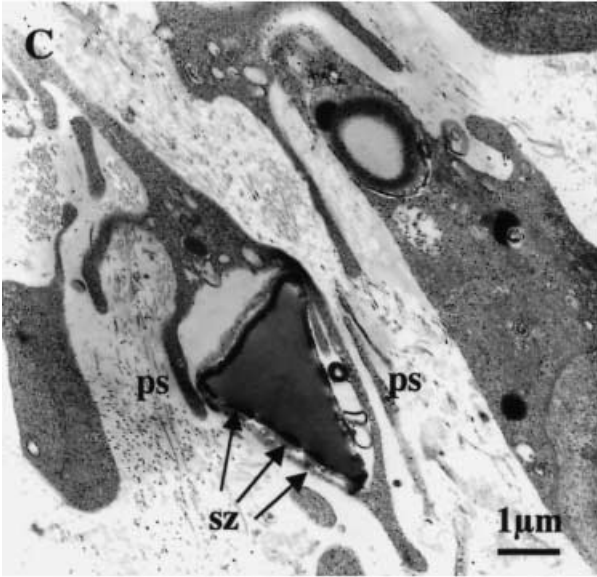
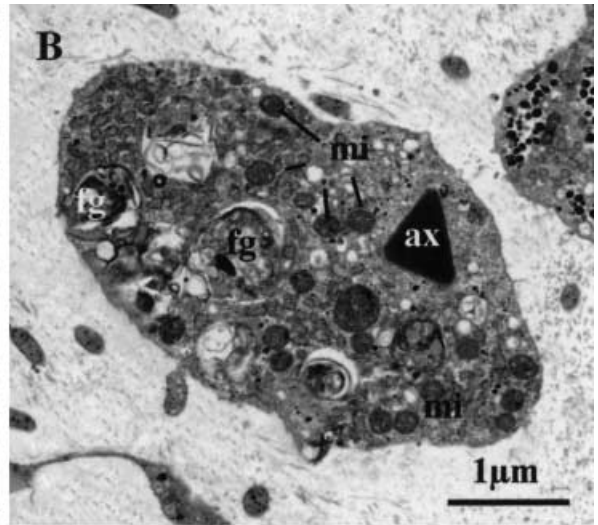
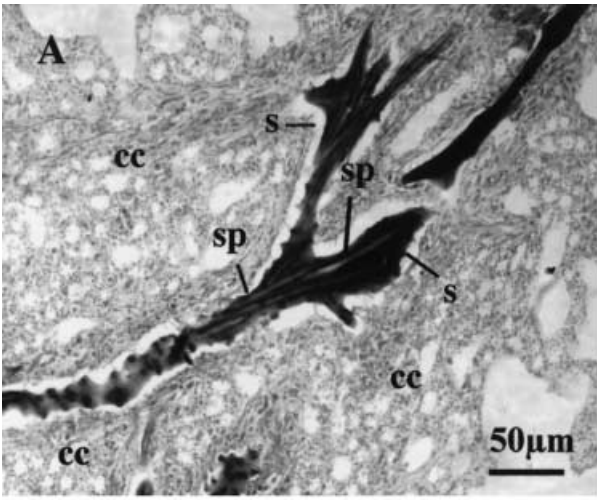
Analyses were performed at high magnification, producing spectra for small areas (3.0, 1.0 and 0.5 µm²). At least three readings were made for archeocytes, spongin, organelles, the cytoplasmic substance within sclerocytes, the space between cells and growing spicules, axial filaments, spicule walls at different stages of the spicule development and perispicular collagen. Significant differences in Si content among the different compartments studied were assessed by one-way ANOVA (data on percentages were Log-transformed prior to the analysis to comply with the assumptions of this parametric procedure).

Results

Ultrastructure

Subtylostyles to styles (200–350 µm × 2–6 µm in size) were the only spicule type present in the specimens of *C.*

Fig. 1 **A** Light micrograph of a sponge section showing ascending spicule bundles surrounded by spongin. **B** TEM image of a sclerocyte containing an axial filament. **C, D** TEM images of sclerocytes enveloping immature spicules at different stages of growth. **E** Larval sclerocyte with a presumably twisted axial filament and yolk reserves. **F** Detail of a connection between the sclerocyte plasmalemma and the membrane surrounding the axial filament or silicalemma. (*ax* Axial filament, *cc* choanocyte chamber, *fg* phagosome, *mi* mitochondria, *ml* multilayered structure, *n* nucleus, *pl* plasmalemma, *ps* pseudopodia, *s* spongin, *sl* silicalemma, *sp* spicule, *sz* Si-rich zones, *v* vesicles, *y* yolk reserves)



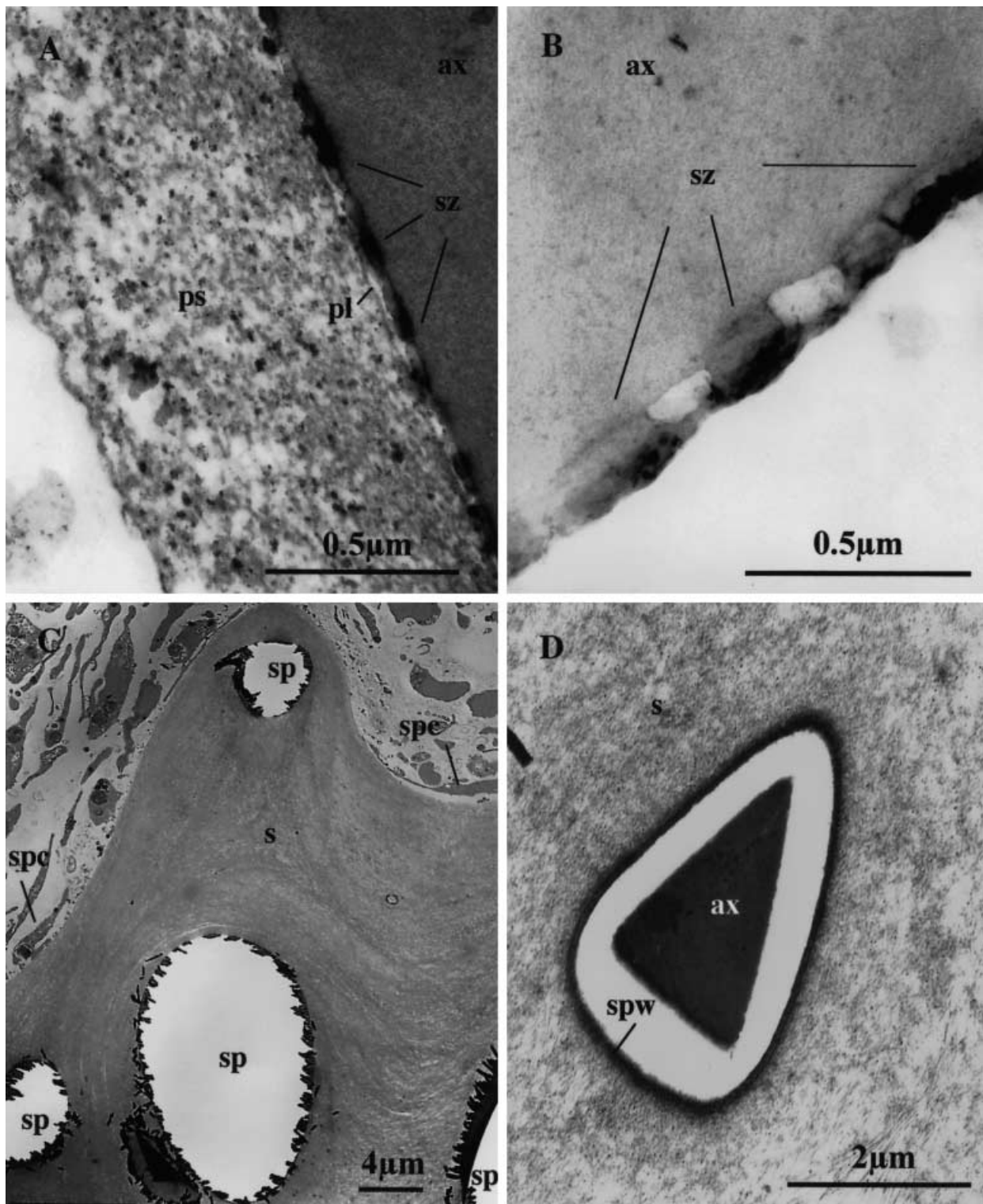


Fig. 2A–D TEM images. **A, B** Early silica deposition; note the regular succession of electron-dense (Si-rich) and electron-clear (Si-poor) zones around the axial filaments. **C** Mature spicules surrounded by a spongin layer produced by peripheral spongocytes (*spe*). **D** Distal point of a mature spicule (note the extremely thin spicule wall, *spw*) surrounded by spongin. Other labelling as in Fig. 1

Fig. 3 **A** Scanning electron-microscopic (SEM) image of a broken spicule showing an axial canal (*ac*) triangular in cross section. **B** TEM photograph of a section of a mature spicule (*sp*) with a triangular shape. **C** Desilicified longitudinal section showing an axial filament (*ax*) and an organic sheath (*sh*). **D, E** Cross and oblique sections, respectively, of desilicified axial filaments showing a central empty core (*c*) corresponding to a Si-rich zone

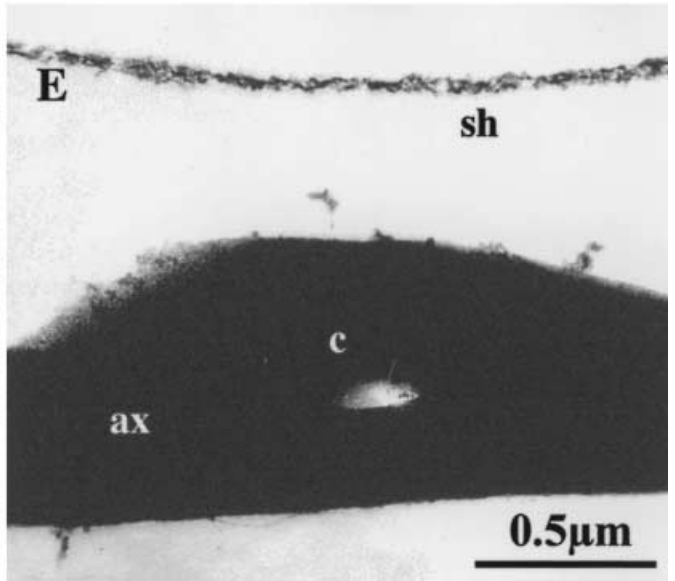
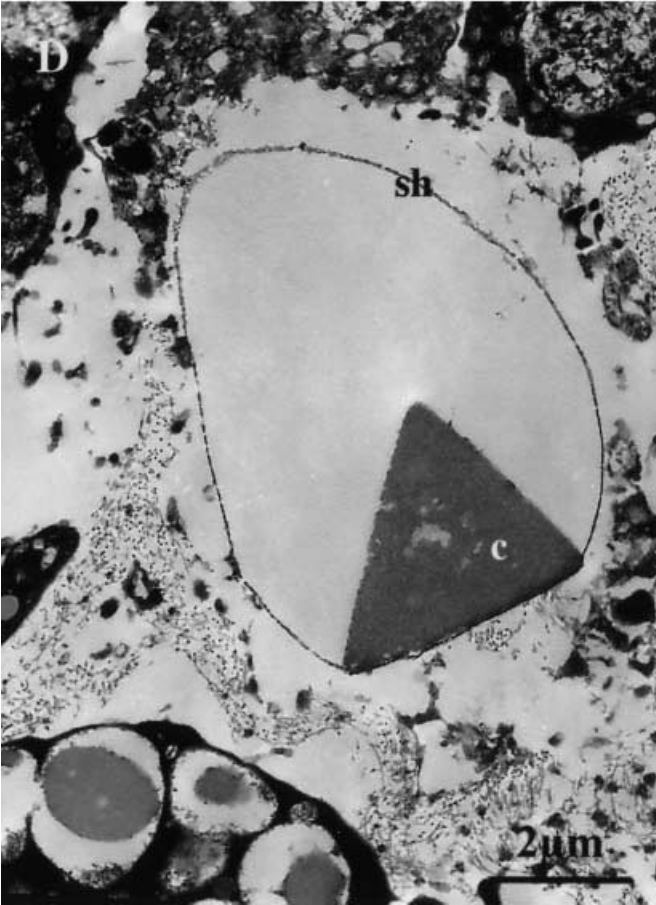
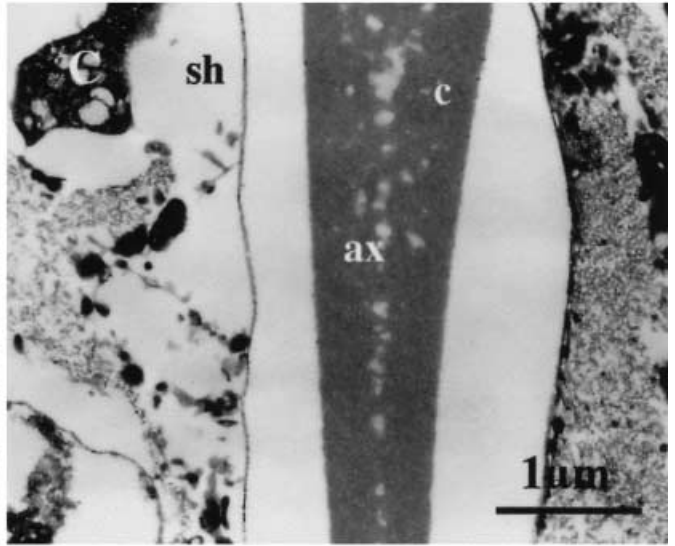
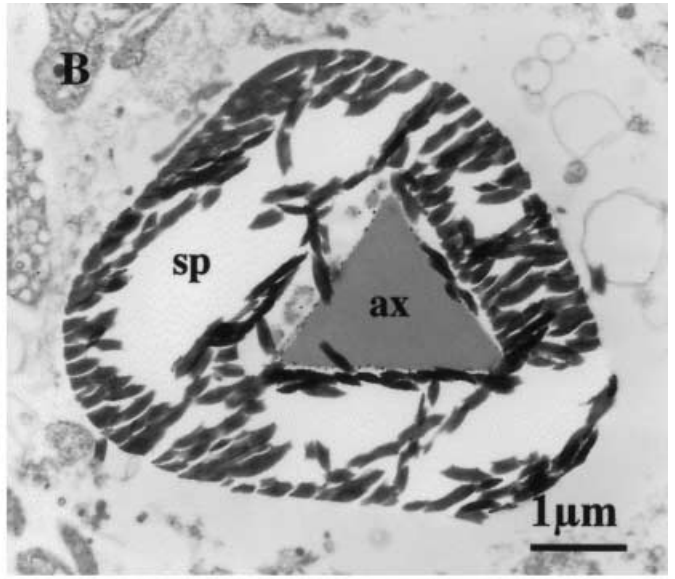
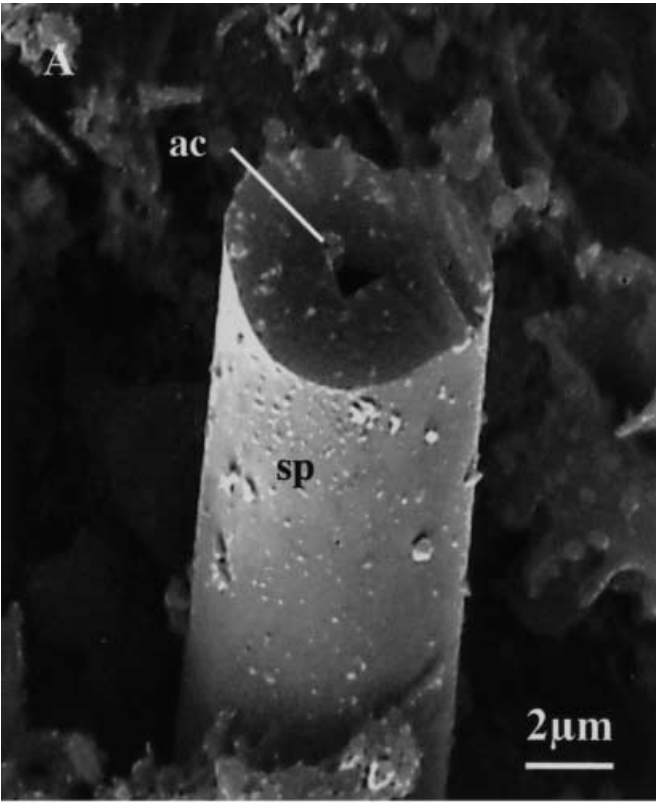
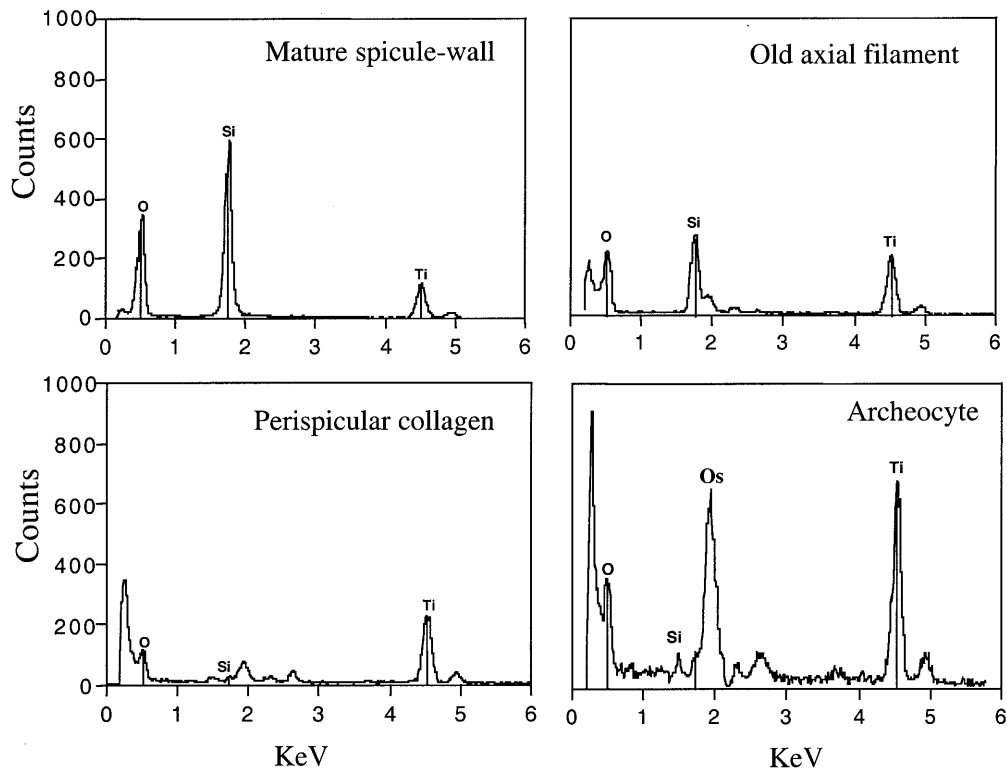


Fig. 4 X-ray microanalysis (XMRA) spectra obtained for mature spicules and archeocytes (Si counts can be standardised against Ti counts in each spectrum)



crambe studied and thus only megasclerocytes were found in the ultrastructural study. Spicules were not abundant and formed ascending bundles from the sponge base towards the upper surface surrounded by spongin (Fig. 1A).

Sclerocytes (megasclerocytes) are 10–12 μm in diameter and have a large nucleolate nucleus, abundant small clear vacuoles, mitochondria and a variable number of phagosomes (Fig. 1B, D, E). No glycogen reserves were conspicuous in these cells even after Thiéry staining. The sclerocytes were occasionally found isolated in the sponge mesohyl but they mainly formed clusters of three to six cells. They were usually seen close to spicules or surrounding them at different stages of growth by means of long thin enveloping pseudopodia (Fig. 1C, D). Axial filaments, 0.7–1.2 μm in diameter, were found within the sclerocytes (Fig. 1B, E). Many instances of free filaments in the sponge mesohyl were also observed, although we could not assess with certainty whether these images corresponded to filaments spontaneously released from the sclerocyte or whether this location was the result of sclerocyte damage during sample processing.

A unit-type membrane surrounding the growing spicule was clearly visible in immature spicules surrounded by the sclerocyte (Figs. 1F, 2A). Moreover, a connection between the cell membrane (plasmalemma) and the membrane that surrounded a growing spicule (called the silicalemma in previous studies) was observed at high magnification (Fig. 1F). It coalesced with the membrane enveloping the spicule. Furthermore, the plasmalemma appeared to concentrate Si in the extracellular space be-

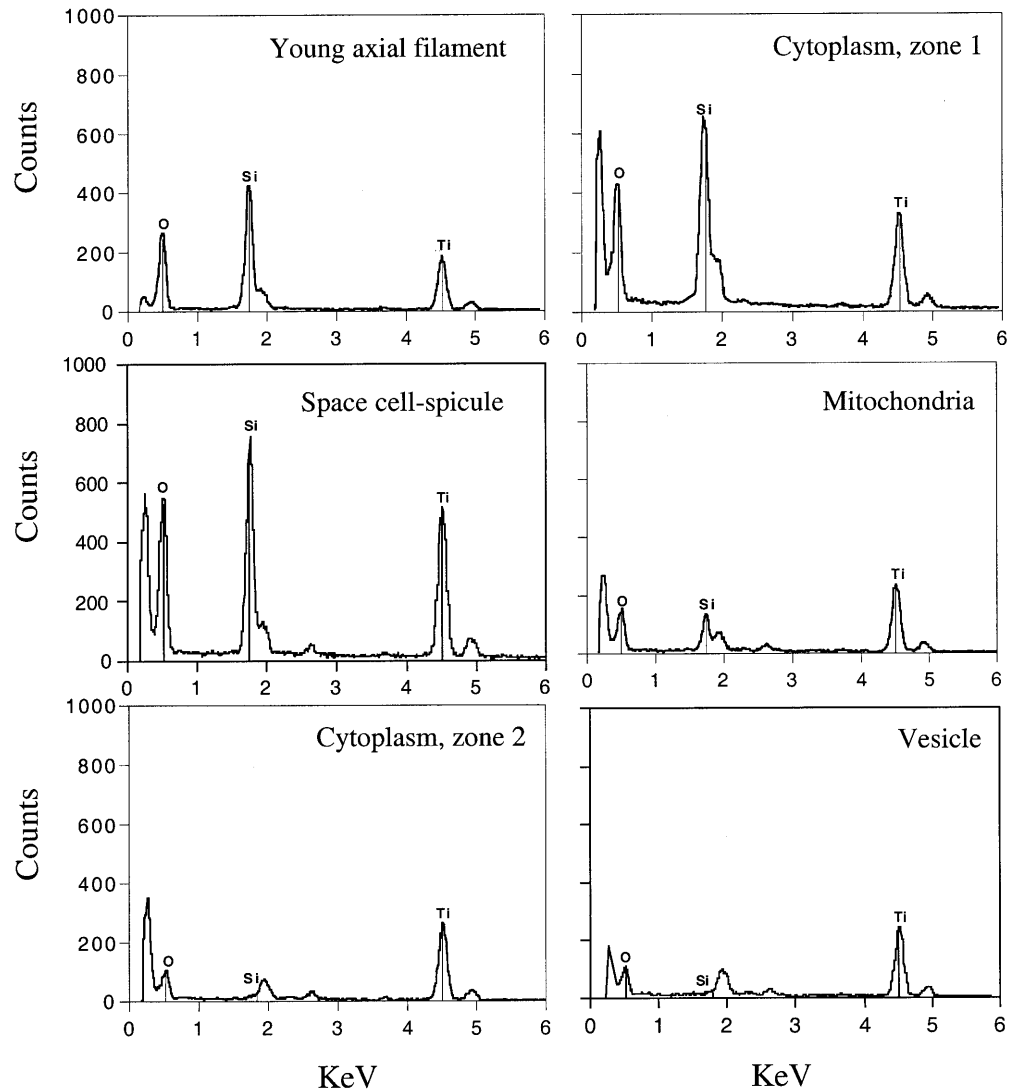
tween the sclerocyte pseudopodia and the growing spicule, according to the data obtained by X-ray analysis (see below).

Larval sclerocytes did not differ from sclerocytes of adult sponges except in the yolk reserves that are characteristic of embryonic stages (Fig. 1E). No growing spicules but only axial filaments were observed in these larvae. The axial filaments were completely included within the sclerocytes. In one instance, two sections, possibly belonging to the same twisted filament were visible within the same sclerocyte (Fig. 1E)

At the beginning of silicification, dense silica-rich zones alternated with clear silica-poor zones at the periphery of the axial filament (Figs. 1C, 2A, B). Mature spicules were not in contact with sclerocytes. Frequently, they were clustered in bundles, enveloped by a dense sheath of collagen-like fibrils of spongin B according to Gross et al. (1956) and surrounded by spongocytes (Fig. 2C). In no case were collencyte-like spicule-carrying cells, as described by Hartman (1981), observed. The cells with pseudopodia always surrounded growing spicules and displayed the typical ultrastructure of sclerocytes.

The diameter of the axial filament ranged from 0.7 μm to 1.7 μm (average 1.1 μm). Completely developed spicules (total diameter ranging from 2 μm at the distal end to 6 μm at the widest zone) showed an axial filament/total spicule diameter ratio of 0.2 at the widest point and 0.7 at the distal end (only cross sections perpendicular to the filament were considered). There was no correlation between filament diameter and total spicule diameter ($r=0.39$, $P=0.15$, $n=15$) in *C. crambe*. The

Fig. 5 XMRA spectra obtained for the various compartments of the growing spicule-sclerocyte complex (Si counts can be standardised against Ti counts in each spectrum)



axial filament appeared to be larger in young spicules than in mature spicules. The instances of a high axial filament/total spicule diameter ratio in mature spicules (i.e. enveloped by spongin) corresponded to transverse sections of the spicule distal point, where the silica layer was much thinner (Fig. 2D).

The axial filament was triangular in the many observed sections, irrespective of whether they had been treated with hydrofluoric acid (Figs. 1B, 2A, C–E, 3B, D). This shape was also observed in cross sections of the axial canal (Fig. 3A) and was even exhibited by some mature spicules (Fig. 3B).

A clearly crystalline structure, such as that described in hexagonal filaments of *Haliclona rosea* (Garrone 1969) and in the microscleres of *Neofibularia irata* (Wilkinson and Garrone 1980) was not seen in axial filaments of *C. crambe* even at the highest magnification used (130,000 \times ; Fig. 1F).

The axial filaments of the samples treated with hydrofluoric acid presented empty spaces in the central part, which indicated that silica was bound to the organic ma-

trix at the centre of the filament (Fig. 3C–E). The presence of silica impregnating the axial filament of growing spicules was also demonstrated by X-ray microanalyses (see below). An organic sheath that surrounded the spicule was always apparent after desilicification (Fig. 3C–E).

X-ray microanalysis

In mature spicules surrounded by spongin, the concentration of Si in the siliceous part of the spicule (hereafter called the spicule-wall) resulted in a Si/Ti ratio of 4.6–6.9. Relatively large amounts of Si were also found in the axial filament (Si/Ti=1.4–2.5) and in the space between the axial filament and the spicule-wall (Si/Ti =1.5). No silica was detected in the perispicular collagen, in archeocytes or in the mesohyl far from the sclerocyte-complex spicule (Si/Ti <0.2 in all cases; Fig. 4).

When sclerocytes secreting spicules were analysed, mitochondria and vesicles, whether electron-dense or

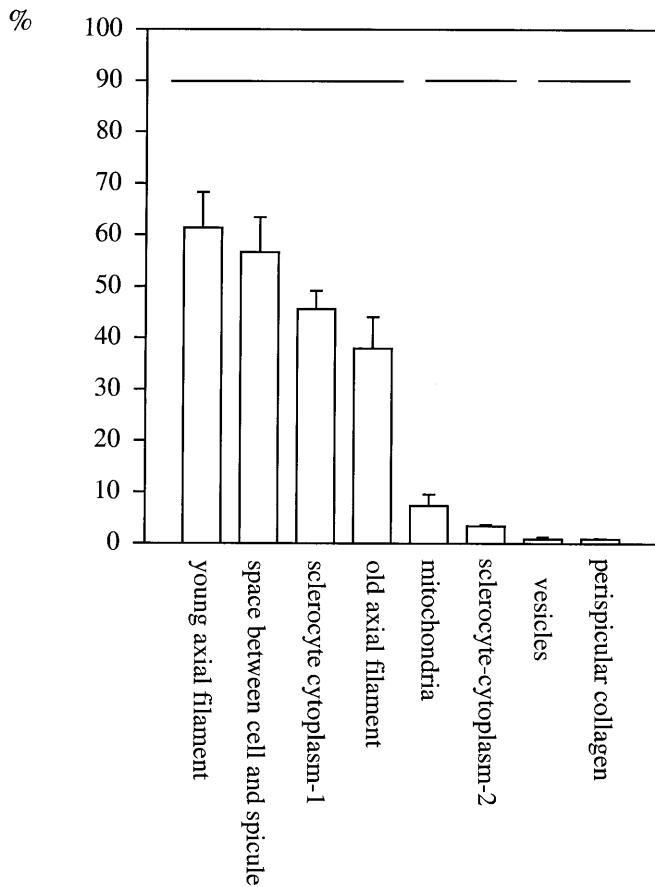


Fig. 6 Si contents (measured as the ratio between the height of the Si $K\alpha$ peak and that of the Ti $K\alpha$ peak) in the various compartments analysed, relative to the Si contained in the wall of a mature spicule (ANOVA $P < 0.0001$, $F = 60.48$, $n = 3$). Three groups, indicated by horizontal bars, contained significantly different amounts of Si (post-hoc test, $P < 0.05$ in all cases)

electron-clear, did not contain significant amounts of silica ($Si/Ti < 0.2$). In contrast, silica was concentrated in the cytoplasm of the pseudopodia that surrounded the growing spicule ($Si/Ti = 2.1$ – 2.39) and in the space between the spicule and the sclerocyte ($Si/Ti = 1$; see Fig. 1C, D). The axial filament of growing spicules contained more silica (Si/Ti up to 3.4) than that of mature spicules (Fig. 5). In short, the axial filament of a growing spicule contained 50%–70% of Si relative to that contained in the spicule-wall, whereas the axial filament of a completely mature spicule only contained 30%–40%. When an extracellular space was visible between the sclerocyte and the growing spicule, the Si content there was 50%–65%. Within the sclerocyte, mitochondria, and vesicles contained about 8% and 2%, respectively. The cytoplasm close to the growing spicule contained up to 50%, whereas the cytoplasm far from the growing spicule only contained less than 5% Si relative to the spicule wall. The ANOVA indicated significant differences in Si content ($F = 60.48$, $n = 3$, $P > 0.001$; Fig. 6) among the various compartments analysed (Fig. 7).



Fig. 7 SEM image of a broken tetraaxial spicule of an Astrophorida sponge (*Stelletta* sp): silica forms concentric layers across the spicule wall, which represent, according to Schwab and Shore (1971a), successive highly hydroxylated surfaces corresponding to pauses in the silicification process

Discussion

Ultrastructural observation coupled with X-ray analysis of the species *C. crambe* has provided key information regarding our understanding of the process of silica deposition in Demosponges. The extracellular growth of megascleres has been demonstrated for the first time and a connection between the plasmalemma and the silica-lemma, which has been presumed in previous studies (Simpson 1984), seems to be present in *C. crambe*, although this requires further verification.

Previous authors conceived the idea that megascleres were formed extracellularly. Simpson (1984) called for caution in accepting that siliceous spicules were in the strict sense intracellular products. Simpson et al. (1985) indicated that it was unlikely that a single cell could cover the entire length of a large megasclere. Calculations performed by these authors showed that the surface area of average-sized sponge cells (10–20 μm in diameter) was about 300–1250 μm^2 , whereas the average surface area of a megasclere of the sponge *S. grubii* was about 80,000–320,000 μm^2 . Thus, these authors concluded that the sclerocytes would have to be giant cells to accommodate intracellular megasclere deposition in this species. However, according to our results, the size

of the megasclere is not the only cause that would determine the extracellular secretion of spicules. Relatively short megascleres, such as those of *C. crambe*, can also be produced extracellularly. In this species, the size of sclerocytes (12 μm in diameter, about 446 μm^2 in area) would allow them to envelop a megasclere (300 μm long, approximately 680 μm^2 in area) almost completely.

As suggested by Simpson (1984), the silicalemma seems to be an invagination of the plasmalemma and silica polymerisation may occur in extracellular pockets. Although a connection of the plasmalemma with the silicalemma has not previously been reported, additional unit-type membranes have been observed in close proximity of the silicalemma (Simpson 1981).

Whether one or several sclerocytes are involved in the formation of a single spicule remains to be demonstrated. The concentric rings observed in cross sections of megascleres of different species (e.g. Fig. 7) corresponding to highly hydroxylated surfaces have been interpreted by Schwab and Shore (1971a) as pauses in silification. These pauses might be the result of a replacement of the sclerocyte that deposits the silica and would allow the siliceous surface to be exposed to the intercellular medium and to become hydroxylated. However, there is no evidence of silification of the same spicule by several sclerocytes, since the cells described as being associated with the sclerocyte-spicule complex (Weissenfels and Landschoff 1977) are, at least in some cases, the spongocytes that secrete the perispicular collagen (Garrone and Pottu 1973).

At the beginning of spicule formation, silica-rich zones (electron-dense) regularly alternate with silica-poor zones (electron-clear) around the axial filament. These silica-rich zones might correspond to active centres of the silicalemma-plasmalemma membrane, as suggested by Davie et al. (1983) and Simpson et al. (1983). However, the regular pattern that they exhibit seems rather to indicate a relationship with the protein structure of the axial filament. Clusters of hydroxy amino acids constitute one of the most distinctive features of silicatein- α , a protein recently identified in the axial filament of sponge spicules (Shimizu et al. 1998) and hydroxyl groups appear to play a role in silica polymerisation. Hydroxyl-rich polysaccharides and oligosaccharides accelerate silica polymerisation in plants (Perry and Lu 1992). Furthermore, hydroxy amino acids are abundant in the proteins associated with the silicified cell walls of diatoms (Swift and Wheeler 1992). Consequently, silica may initially be concentrated in these hydroxylated zones of the axial filament to produce the pattern observed. This pattern of silica deposition supports the "deposition-distribution" theory of Simpson (1989), which assumes the continuous mobility of silicic acid or its dimer or trimer derivatives within the silicalemma and provides an acceptable explanation for the uniformity of the shape of the spicule along its length. The alternative theory (Simpson 1989) presupposes the direct control of the transport rate across the whole surface of the silicalemma-

plasmalemma membrane; this seems to be a more complicated mechanism.

The transport of spicules by cells has been recorded in both marine and freshwater sponges (Elvin 1971; Bond and Harris 1988; Bond 1992) and has also been documented for freshwater sponges by time-lapse video (TokyoCinema 1996). However, in these cases, the carrying cells involved have not been identified. In *Ephydatia muelleri*, sclerocytes containing growing spicules have been observed wandering quickly through the sponge mesohyl (Elvin 1971). Our results based on electron-microscopic images are consistent with Elvin's (1971) observation by light microscopy. In *C. crambe*, only sclerocytes appear to be involved in spicule transportation, since only sclerocytes have been found in contact with spicules in the many sections observed. These sclerocytes appear to carry young spicules as they are completing silica deposition, since no instances of sclerocytes surrounding mature spicules have been observed.

If the interpretation of previous authors regarding spicule secretion is correct, megasclere formation in Demosponges could occur both intra- and extracellularly, depending on the spicule type. Thus, large or elaborate megascleres might be secreted extracellularly, whereas the secretion of the small megascleres of Halicionid and Spongillid sponges and most microscleres may be intracellular. An odd case is the extracellular or intracellular origin of the toxes of *Microciona*, depending on the species (Simpson 1968).

The response of microsclerocytes to changes in silicic acid concentration is different from that of megasclerocytes in experimental cultures of *Spongilla lacustris* (Jorgensen 1944). This might depend on whether the mechanism of silification is extra- or intracellular. A recent experiment with settlers of *C. crambe* cultured in the laboratory (Maldonado et al. 1999) has shown that concentrations of silicic acid as low as those of the Mediterranean littoral do not allow the formation of microscleres and only megascleres are secreted. In contrast, at higher concentrations, a profusion of microscleres (isochelae and asteroid desmas) is produced under laboratory conditions. Thus, megasclerocytes are better competitors for silica than microsclerocytes in *C. crambe*; this different capability might depend on whether silica is deposited inside or outside the cell.

Axial filaments of *C. crambe* are wider than those previously described for other sponges. Their diameter ranges from 0.7 μm to 1.7 μm (average 1.1 μm) vs 0.41–0.60 μm in the Poecilosclerid *Acarnus erithaceus* (Schwab and Shore 1971a, 1971b) and 0.66–1.00 μm in the Astrophorid *S. grubei* (Simpson et al. 1985; from cross sections of desilicified megascleres). No positive correlation between filament and spicule diameter seems to exist across species, i.e. the spicules of *C. crambe* are up to 350 μm long and have larger axial filaments than the spicules of *S. grubii*, which are up to 2000 μm long (Uriz 1981; Simpson et al. 1985).

The axial filament of the spicules of *Crambe crambe*, both before and after desilicification, is in all instances

triangular in cross section as are the axial canal and the shape of growing spicules. The angles of the triangle may be rounded because of filament retraction or spontaneous silica dissolution in old spicules. The same process may have produced the "hexagonal" profiles described in the triaenes and oxeas of *S. grubii* (Simpson et al. 1985). Treatment with hydrofluoric acid appears to affect the form of the axial filament in the latter species, in which the filament is highly impregnated by silica. However, the "hexagonal" images are poorly defined and are quite different from the clearly hexagonal cross sections illustrated for species of Haplosclerida (Garrone 1969); these also show a crystalline structure. The rounding of the angles of the triangular filaments observed in old spicules of *C. crambe* makes the hypothesis of Garrone (communicated to Simpson 1989) unlikely. This hypothesis postulates that a triangular cross section develops directly by differential growth of the faces of a hexagon.

Consequently, axial filaments that are triangular in cross section would lie at the base of the four-polyaxial spicules, independently of whether this potential morphology is expressed (Simpson et al. 1985), as stated by Reischwig (1971). Instances of the phenotypic non-expression of polyaxial morphology can be found in Hadromerida (Rützler and Smith 1993) and in some Poecilosclerida, such as *Crambe* and *Discorhabdella* (Uriz and Maldonado 1995). This polyaxial morphology might also be consistent with the extracellular silica deposition of megascleres but the extracellular secretion of the tetraxon spicules in Astrophorid sponges with triangular filaments has to be established before any generalisations can be proposed. The shape of the axial filament was unresolvable in most Halichondrida examined by Reischwig (1971), although the author suspected that it was not triangular. Ultrastructural studies of Halichondrid species are needed before the possible taxonomic significance of this character can be ascertained for all Demosponges.

The presence of an internal silicified core in the axial filament of megascleres (Garrone 1969; Simpson et al. 1985) has been confirmed from observations of an empty central zone in filaments of *C. crambe* spicules following desilicification. Moreover, relatively large amounts of Si have been detected in the axial filament of young spicules by X-ray analyses, indicating the presence of silica.

To summarise, megasclere secretion takes place in *C. crambe* extracellularly. Once the axial filament is extruded to the mesohyl, silicification is accomplished in an extracellular space delimited by the sclerocyte pseudopodia. The silicella appears to be nothing other than the plasmalemma, as suggested by Simpson (1984). According to the results from the microanalyses, Si appears to be concentrated in the cytoplasm of the sclerocyte close to the growing spicule. It may be transferred from the sclerocyte to the perispicular space through the cell plasmalemma.

Acknowledgements The authors are indebted to the Microscopy Service Staff of the University of Barcelona for assistance with scanning- and transmission electron microscopy and microanalysis. They also thank N. Boury-Esnault and T. Simpson for fruitful comments on the manuscript, and G. Agell for help in figure processing.

References

- Andral B, Stanisiere JY, Sauzade D, Henocque Y, Thebault H, Boissery P (1998) Étude des niveaux de contamination chimique en Méditerranée basée sur l'utilisation de stations artificielles de moules. *Rapp Comm Int Mer Médit* 35:224–225
- Angelidis MO, Aloupi M (1998) Evaluation of metal pollution in the coastal sediments of Lesbos Island, Aegean sea. *Rapp Comm Int Mer Médit* 35:226–227
- Bei F, Catsiki VA, Stroglyoudi E (1998) Seasonal and spatial variation of Cu, Cr, Ni and Pb concentrations in *Mytilus galloprovincialis* of Saronikos Gulf, Greece. *Rapp Comm Int Mer Médit* 35:230–231
- Bibiloni MA (1990) Fauna de Esponjas de las Islas Baleares. Variación cualitativa y cuantitativa de la Población de esponjas en un gradiente batimétrico. Comparación Baleares-Costa Catalana. Ph.D. thesis, Universidad de Barcelona
- Bogner D, Juracic M, Baric A (1998) Strand Ni content in sediments from Kastela Bay, Adriatic Sea, Croatia. *Rapp Comm Int Mer Médit* 35:232–233
- Bond C (1992) Continuous cell movements rearrange anatomical structures in intact sponges. *J Exp Zool* 263:284–302
- Bond C, Harris AK (1988) Locomotion of sponges and its physical mechanism. *J Exp Zool* 246:271–284
- Boury-Esnault N, Doumenc DA (1979) Glycogen storage and transfer in primitive invertebrates: Demospongia and Actinaria. In: Lévi C, Boury-Esnault N (eds) *Biologie des spongiaires*. *Sponge Biology*. Centre National de la Recherche Scientifique, Paris, pp 181–192
- Chapple JP, Smerdon GR, Hawkins AJS (1997) Stress-70 protein induction in *Mytilus edulis*: tissue-specific responses to elevated temperature reflect relative vulnerability and physiological function. *J Exp Mar Biol Ecol* 217:225–235
- Davie EI, Simpson TL, Garrone R (1983) Experimental germanium incorporation into siliceous sponge spicules. *Biol Cell* 48:191–201
- Elvin D (1971) Growth rates of the siliceous spicules of the freshwater sponge *Ephydatia muelleri* (Lieberkühn). *Trans Am Microsc Soc* 90:219–224
- Garrone R (1969) Collagène, spongine et squelette minéral chez l'éponge *Haliciona rosea* (O.S.) (Demosponge, Haploscléride). *J Microsc* 8:581–598
- Garrone R, Pottu J (1973) Collagen biosynthesis in sponges: Elaboration of spongin by spongocytes. *J Submicrosc Cytol Pathol* 5:199–218
- Garrone R, Simpson TL, Pottu J (1981) Ultrastructure and deposition of silica in sponges. In: Simpson TL, Volcani BE (eds) *Silicon and siliceous structures in biological systems*. Springer, Berlin Heidelberg New York, pp 495–525
- Gross HJ, Sokal Z, Rougvie M (1956) Structural and chemical studies on the connective tissue of marine sponges. *J Histochem Cytochem* 4:227–246
- Hartman WD (1981) Form and distribution of silica in sponges. In: Simpson TL, Volcani BE (eds) *Silicon and siliceous structures in biological systems*. Springer, Berlin Heidelberg New York, pp 453–493
- Jorgensen CB (1944) On the spicule-formation of *Spongilla lacustris* (L.). 1. The dependence of the spicule-formation on the content of dissolved and solid silicic acid of the milieu. *Det Kgl Danske Vidensk Selsk Biol Medd* 19:2–45
- Ledger PW (1975) Septate junctions in the calcareous sponge *Sycon ciliatum*. *Tissue Cell* 7:13–18

- Ledger PW, Jones WC (1991) On the structure of calcareous sponge spicules. In: Reitner J, Keupp H (eds) Fossil and recent sponges. Springer, Berlin Heidelberg New York, pp 341–359
- Maldonado M, Uriz MJ (1996) Skeletal morphology of two controversial Poecilosclerid genera (Porifera, Demospongiae): *Discorhabdella* and *Crambe*. *Helg Meeres* 50:369–390
- Maldonado M, Carmona MC, Uriz MJ, Cruzado A (1999) Decline in Mesozoic reef-building sponges explained by silicon limitation. *Nature* 401:785–788
- Perry CC, Lu Y (1992) Preparation of silicas from silicon complexes: role of cellulose in polymerisation and aggregation control. *J Chem Soc Faraday Trans* 88:2915–2921
- Reiswig HM (1971) The axial symmetry of sponge spicules and its phylogenetic significance. *Cah Biol Mar* 12:505–514
- Reynolds ES (1963) The use of lead citrate at high pH as an electron-opaque stain in electron microscopy. *J Cell Biol* 17:208–212
- Rützler K, Smith KP (1993) The genus *Terpios* (Suberitidae) and new species in the “Lobiceps” complex. In: Uriz MJ, Rützler K (eds) Recent advances in ecology and systematics of sponges. Scientia Marina, Barcelona, Spain, pp 381–393
- Schwab DW, Shore RE (1971a) Fine structure and composition of a siliceous sponge spicule. *Biol Bull* 140:125–136
- Schwab DW, Shore RE (1971b) Mechanism of internal stratification of siliceous sponge spicules. *Nature* 232:501–502
- Shimizu K, Cha JH, Stucky GD, Morse DE (1998) Silicatein alpha: cathepsin L-like protein in sponge biosilica. *Proc Natl Acad Sci USA* 95:6234–6238
- Simpson TL (1968) The structure and function of sponge cells: new criteria for the taxonomy of Poecilosclerid sponges (Demospongiae). *Peabody Mus Nat Hist (Yale Univ)* 25:1–141
- Simpson TL (1981) Effects of germanium on silica deposition in sponges. In: Simpson TL, Volcani VE (eds) Silicon and siliceous structures in biological systems. Springer, Berlin Heidelberg New York, pp 527–550
- Simpson TL (1984) The cell biology of sponges. Springer, Berlin Heidelberg New York
- Simpson TL (1989) Silification processes in sponges: *Geodia asters* and the problem of morphogenesis of spicule shape. In: Crick RE (ed) Origin evolution, and modern aspects of biomineralization in plants and animals. Plenum, New York, pp 125–136
- Simpson TL, Vaccaro CA (1974) An ultrastructural study of silica deposition in the fresh water sponge *Spongilla lacustris*. *J Ultrastr Res* 47:296–309
- Simpson TL, Garrone R, Mazzorana M (1983) Interaction of germanium (Ge) with biosilification in the freshwater sponge *Ephydatia muelleri*: evidence of localized membrane domains in the silicalemma. *J Ultrastruct Res* 85:159–174
- Simpson TL, Langenbruch PF, Scalera-Liaci L (1985) Silica spicules and axial filaments of the marine sponge *Stelletta grubii* (Porifera, Demospongiae). *Zoomorphology* 105:375–382
- Spurr AR (1969) A low-viscosity epoxy resin embedding medium for electron microscopy. *J Ultrastr Res* 26:31–43
- Swift DM, Wheeler AP (1992) Evidence of an organic matrix from diatom biosilica. *J Phycol* 28:202–209
- Thiele J (1899) Ueber *Crambe crambe* (O. Schmidt). *Arch Naturgesch* :87–94
- Thompson JE, Barrow KD, Faulkner DJ (1983) Localization of two brominated metabolites aethionin and homoethionin, in sphaerulous cells of the marine sponge *Aplysina fistularis* (= *Verongia thiona*). *Acta Zool Stockh* 64:199–210
- TokyoCinema (1996) Life of the freshwater sponge. TokyoCinema, Tokyo
- Uriz MJ (1981) Estudio sistemático de las esponjas *Astrophorida* (Demospongia) de los fondos de pesca de arrastre, entre Tossa y Calella (Cataluña). *Bol Inst Esp Oceanogr* 6:7–58
- Uriz MJ, Maldonado M (1995) A reconsideration of the relationship between polyaxonid and monaxonid spicules in Demospongiae: new data from the genera *Crambe* and *Discorhabdella* (Porifera). *Biol J Linnean Soc* 55:1–15
- Uriz MJ, Rosell D, Martín D (1992) The sponge population of the Cabrera Archipelago (Balearic Islands): characteristics, distribution, and abundance of the most representative species. *PSZN Mar Ecol* 13:101–117
- Weissenfels N, Landschoff HW (1977) Bau und Funktion des Süßwasserschwammes *Ephydatia fluviatilis* L. (Porifera). IV. Die Entwicklung der Monaxialen SiO₂ Nadeln in Sandwich-Kulturen. *Zool Jb Anat Bd* 98:355–371
- Weissenfels N, Langenbruch PF (1985) Langzeitkulturen von Süßwasserschwämmen (Porifera, Spongillidae) unter Laborbedingungen. *Zoomorphology* 105:12–15
- Wilkinson CR, Garrone R (1980) Ultrastructure of siliceous spicules and microsclerocytes in the marine sponge *Neofibularia irata* n. sp. *J Morphol* 166:51–64